

## DYNAMIC RESPONSE OF THE SHIP AND THE BERTHING FENDER SYSTEM AFTER IMPACT

*By Sadao KOMATSU\* and Abdel Hamid SALMAN\*\**

### ABSTRACT

This paper describes a method of analysis for evaluating the portion of ship kinetic energy and impact force transmitted to a berthing structure provided with fenders which have linear or non-linear spring constants. In the analysis, presented herein, the dynamic responses of the ship, fender and berthing structure, after impact, are considered, and derived equations for the selection of different parameters needed for the solutions of the dynamic equations are included. These are comprised of the virtual mass of the ship, in both translational and rotational motion, in addition to the time interval required for the solutions of the motion equations by numerical integration methods.

### 1. INTRODUCTION

Since the size of ships, particularly tankers, has increased in recent years, the design of offshore berthing structures has become more important. One of the prime difficulties facing designers is the evaluation of the portion of ship kinetic energy and the impact force transmitted to each of the fenders and the berthing structure, especially structures provided with rubber-like fenders.

#### (1) The Kinetic Energy of the Berthing Ship

When a ship is approaching the berth with both translational and rotational motion, its kinetic energy is given by the following equation;

$$E_0 = \frac{1}{2} M_2 V_0^2 + \frac{1}{2} I_G \omega_0^2 \quad \dots\dots(1)$$

where  $M_2$  = virtual mass of the ship,  
 $I_G$  = virtual moment of inertia about the vertical axis through the ship's center of gravity,  
 $V_0$  = velocity of translation,  
 $\omega_0$  = angular velocity.

#### (2) The Effective Energy for Fender System Design

During berthing the kinetic energy of the ship may be dissipated in several ways, among which are the following:

- i) Elastic deformation of the structure and fender.
- ii) Swinging of the ship due to yawing motion.
- iii) Heeling of the ship due to rolling motion.
- iv) Elastic deformation of the ship's hull.
- v) Piling of the water trapped between the ship's hull and the face of the berthing structure. (This occurs in the case of a long closed structure.)

Designers who are involved with marine structures design are interested in the portion of energy indicated by i) which is called the effective energy ( $E_e$ ). The problem of determining the effective energy has been treated analytically by several investigators. Michalos<sup>1),2)</sup> treated the problem as one which had a single-degree-of-freedom dynamic motion, and considered the theory of elastic impact in his analysis. The judgement of others<sup>3),4)</sup>, including the authors, is that the ship's dynamic impact on the structure can be considered as a plastic impact, where, upon impact, both the ship and the fender system move together as one combined mass. Vasco Costa<sup>5)</sup> has derived a dynamic equation for estimating the effective energy in which only the portion of the energy dissipated by the yawing motion of the ship was considered. The rolling motion and the influence of the fender system dynamic response were ignored. Hayashi and Shirai<sup>6)</sup> have dealt with the problem as one which

\* Professor of Civil Engineering, Osaka University.

\*\* Doctorate Course Student, Civil Engineering Department, Osaka University (Eng. Suez Canal Research Center, Egypt).

has three-degrees-of-freedom dynamic motion; swaying, yawing, and rolling motion. The equations are valid i) for structures which are provided with linear spring constants, such as steel spring-like fenders. ii) for only one case of approaching mode of berthing, in which the vector of the approaching velocity is perpendicular to the arm connecting the ship's center gravity with the point of contact.

Besides, the dynamic response of the fender system was ignored. The empirical equation for determining the effective energy ( $E_e$ ) is also used for design purposes and is of the form

$$E_e = CE_0 \quad \dots\dots(2)$$

where  $E_0$  represents the approaching ship's kinetic energy and  $C$  is the reduction or dispersion factor. Pages<sup>18)</sup> suggests the following equation for determining for  $C$ ;

$$C = 1/(1 + 16a^2) \quad \dots\dots(3)$$

where  $a = d/L$ .  $L$  represents the ship's total length and  $d$  represents the distance between the ship's center of gravity and the point of contact, measured parallel to the berthing face. Other designers have selected a value of  $C$  which varies from 0.2 to 1.0 depending on several factors, such as the mode of berthing operation, local hull deformation, structure type, etc.<sup>2), 6), 7), 18)</sup>

From published information it became clear that the portion of the energy transmitted separately to the berthing structure and fender is

still a problem, especially in the case of fenders with non-linear spring constants, and rubber-like fenders, which are in this class, are being used extensively due to their large energy-absorbing characteristics.

The authors have presented a method of analysis based on the dynamic behavior of the system, after collision, to evaluate the impact load and the portion of the ship's kinetic energy transmitted to the berthing structure and fenders which includes fenders that have both linear and non-linear spring constants. Also, to evaluate the portion of the energy dissipated in the swinging and rolling of the ship after impact.

## 2. DYNAMIC RESPONSE OF THE SHIP AND THE BERTHING STRUCTURE AFTER THE FIRST IMPACT

### (1) General Mode of Berthing

When the ship is approaching the berth under its own power, it is angled in to make the first contact with the fender system at a point near its bow or stern. This point of contact is always located in a horizontal plane higher than that passing through the ship's center of gravity. During this mode of berthing, the ship will undergo dynamic motion which has three-degree-of-freedom, namely; swaying, yawing, and rolling. The other motions, heaving, pitching and

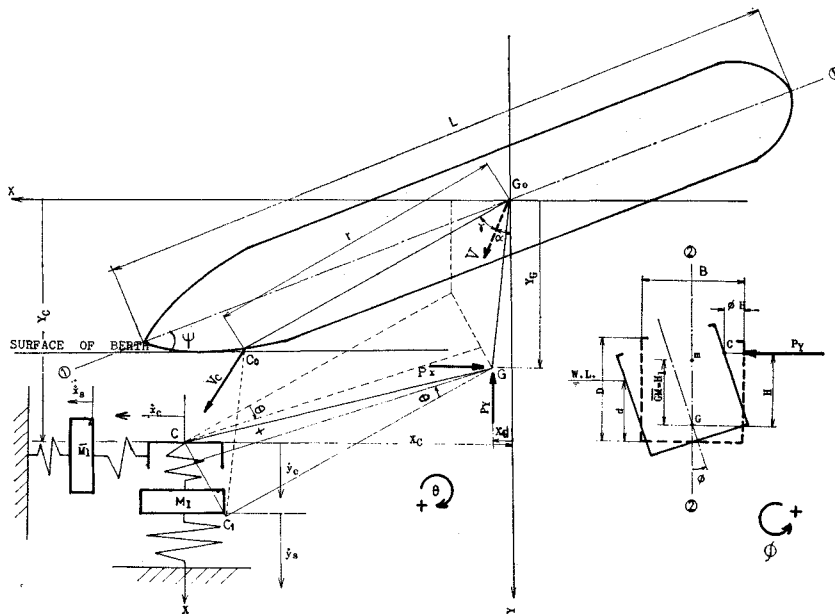


Fig. 1 Behaviour of ship after contact.

surging are of little consequence in energy dissipation and may be neglected.

(2) Equations of Motion

In the following analysis it is assumed that no sliding contact is made along the fender's surface.

Consider the motion of the ship, as a free body under the action of the load  $P$  acting at the point of contact  $C$ , we have;

At any time  $t$ , after the ship came in contact with the fender system, Fig. 1, its center of gravity will sway in the direction of the acting load, to the position  $G$ . Then the ship will swing about its vertical axis passing through  $G$ , an angle  $\theta$  due to the yawing motion and finally it will roll about its horizontal longitudinal axis an angle  $\phi$ . Denote the coordinates of the final positions of  $G$  and  $C$ , with respect to the axes  $X$  and  $Y$ , by  $(X_G, Y_G)$  and  $(X_C, Y_C)$  respectively. The  $X$  and  $Y$  axes are taken parallel and normal to the surface of berthing respectively. From the figure, the relation connecting the fender system motion at  $C$  with the motion of  $G$  is;

$$\left. \begin{aligned} \ddot{X}_C &= \ddot{X}_G + (r\ddot{\theta} + H\ddot{\phi}) \cos(\gamma + \alpha) \\ \ddot{Y}_C &= \ddot{Y}_G - (r\ddot{\theta} + H\ddot{\phi}) \sin(\gamma + \alpha) \end{aligned} \right\} \dots\dots(4)$$

the second order terms in the above equation,  $\dot{\theta}^2, \dot{\phi}^2$  are neglected.

Consider the dynamic equilibrium of  $G$ , the following equations of motion will hold;

$$\left. \begin{aligned} \text{i) SWAY} \\ M_2 \ddot{X}_G &= -P_X - R w_X \\ M_2 \ddot{Y}_G &= -P_Y - R w_Y \\ \text{ii) YAWING} \\ I_{2-2} \ddot{\theta} &= P_Y \cdot r \cdot \sin(\gamma + \alpha) \\ &\quad - P_X \cdot r \cdot \cos(\gamma + \alpha) - N_1 \\ \text{iii) ROLLING} \\ I_{1-1} \ddot{\phi} &= (P_Y \cdot \cos \phi - P_X \cdot \sin \phi) H \\ &\quad - W \cdot H_1 \cdot \phi - N_2 \end{aligned} \right\} \dots\dots(5)$$

$P_X, P_Y$  and  $R w_X, R w_Y$  are the components of the fender reaction and the water resistance, after the ship came in contact with the fender system, respectively.  $N_1$  and  $N_2$  denote the water resistance to yawing and rolling motions respectively. However, as the time of contact is very small, water resistance, is safely allowed. Water resistance is effective in the time between the first and the second impact, this will be discussed in details in next paper.

As for the berthing structure response, the following eq. will hold;

$$\left. \begin{aligned} M_1 \ddot{X}_s &= P_X - K_X \cdot X_s - \mu_X \cdot \dot{X}_s \\ M_1 \ddot{Y}_s &= P_Y - K_Y \cdot Y_s - \mu_Y \cdot \dot{Y}_s \end{aligned} \right\} \dots\dots(6)$$

In the previous equations the value of  $P$  is evaluated from the given load-deflection relation ( $P-D$ ) of the fender in question. The load is considered to be applied in small increments associated with the time interval. This  $P-D$  relation is determined from statical analysis or tests. At any time  $t$ , the deflection  $D$  will be calculated from the displacement of the point of contact  $C$  and the deflection of the structure, which will equal to;

$$\left. \begin{aligned} D_X &= X_C - X_s \\ D_Y &= Y_C - Y_s \end{aligned} \right\} \text{ and } D = \sqrt{D_X^2 + D_Y^2} \dots\dots(7)$$

In considering the second impact, the velocity of the point of the first contact at separation, magnitude and direction is needed, which will equal to;

$$\left. \begin{aligned} V_C &= \sqrt{\dot{X}_C^2 + \dot{Y}_C^2} \\ \alpha_t &= \tan^{-1}(\dot{X}_C / \dot{Y}_C) \end{aligned} \right\} \dots\dots(8)$$

At time of contact  $\alpha_{t0} = \alpha$ , the angle that the approaching velocity makes with  $Y$ -axis.  $\alpha$  is considered positive when the velocity vector of  $V_0$  at  $G$  points towards the point of contact  $C$ .

If the value of the spring constant of the ship hull at point of contact is available, the elastic deformation of the ship's hull can be evaluated. Let  $K_h, S_h,$  and  $\mu_h$  define the spring constant, deflection, and the damping coefficient of the hull at point of contact respectively, then the equation of deflection of the ship's hull, in  $P$ -direction, will be;

$$\ddot{S}_h = (P - K_h \cdot S_h - \mu \cdot \dot{S}_h) \dots\dots(9)$$

In this case  $P$  will be function of  $(X_C, Y_C, X_s, Y_s, S_h)_t$ . The initial conditions of motion, at time of contact, are;

$$\left. \begin{aligned} X_G = Y_G = \theta = \phi = X_C = Y_C \\ = X_s = Y_s = S_h = 0.0 \\ \dot{X}_G = \dot{X}_C = V_0 \sin \alpha \\ \dot{Y}_G = \dot{Y}_C = V_0 \cos \alpha \\ \dot{\theta} = \dot{\phi} = \dot{X}_s = \dot{Y}_s = \dot{S}_h = 0.0 \end{aligned} \right\} \dots\dots(10)$$

The solution of dynamic equations is carried out by numerical integration methods with the help of the digital computer.

(3) Energy Equations

The developed previous equations are valid as long as the ship being in contact with the fender. During this time, the following energy equations are valid;

$$\begin{aligned}
 & \text{I. Part of the ship's kinetic energy transmitted to;} \\
 & \left. \begin{aligned}
 & \text{i) Fender} \quad V_f = \int^t P \cdot dD_t \\
 & \text{ii) Structure} \quad V_s = \int^t K_s \cdot dS_t \\
 & \text{iii) Ship's Hull} \quad V_h = \int^t K_h \cdot dS_{h_t} \\
 & \qquad \qquad \qquad = \text{effective energy } E_e
 \end{aligned} \right\} \\
 & \text{II. Work done by the ship in rotational motions;} \\
 & \left. \begin{aligned}
 & \text{i) Swinging} \quad W_s = \int^t P \cdot r \cdot d\theta_t \\
 & \text{ii) Heeling} \quad W_h = \int^t P \cdot H \cdot d\phi_t
 \end{aligned} \right\} \\
 & \text{III. Part of energy induced in the system vibration;} \\
 & \left. \begin{aligned}
 & \text{i) Ship} \quad E_{sh} = \frac{1}{2} M_2 (\dot{X}_G^2 + \dot{Y}_G^2) \\
 & \qquad \qquad \qquad + \frac{1}{2} I_{2-2} \dot{\theta}^2 + \frac{1}{2} I_{1-1} \dot{\phi}^2 \\
 & \text{ii) Structure} \quad E_s = \frac{1}{2} M_1 (\dot{X}_s^2 + \dot{Y}_s^2)
 \end{aligned} \right\} \dots\dots(11)
 \end{aligned}$$

The above equations should satisfy the conservation of energy during berthing *i.e.*

$$E_0 = \frac{1}{2} M_2 V_0^2 = E_e + E_{sh} + E_s \quad \dots\dots(12)$$

**(4) Broadside Berthing**

If the motion of the ship during the berthing operation is mainly governed by tugboats, as is always the case with the large ships, the ship can make contact with the berthing structure entirely broadside. In this case the ship will undergo dynamic motion which has two-degree-of-freedom; swaying and rolling, and terms containing  $\theta$  in equations (5) and (11) with vanish.

If the energy dissipated by rolling motion is neglected for safety, then the fender system will be designed to absorb all of the kinetic energy of the ship, which is the case when  $C=1.0$  in equation (2). This mode of berthing is considered ideal as the ship impact load will be uniformly distributed on the structure<sup>18)</sup>.

If we assume that the berthing structure is provided with a fender which has a linear spring constant  $K_f$  the equations of motion will be;

$$\text{i) Structure} \quad \left. \begin{aligned} & \dot{Y}_s = (P - K_s \cdot Y_s - \mu \cdot \dot{Y}_s) / M_1 \end{aligned} \right\} \dots\dots(13)$$

$$\text{ii) Ship (+fender)} \quad \left. \begin{aligned} & \dot{Y}_c = -P / M_2 \end{aligned} \right\}$$

in which  $P = K_f(Y_c - Y_s)$  and  $Y_s, Y_c$  are the displacements of the structure and the point of contact respectively in  $Y$ -direction Fig. 1.

If, at the time of contact, the following conditions exist;

$$Y_s = Y_c = 0.0 \quad \dot{Y}_s = 0.0 \quad \dot{Y}_c = V_0 \quad \dots\dots(14)$$

and assuming  $\mu = 0.0$ , the analytical solution of these eq. (13) is given by;

$$\left. \begin{aligned} Y_s &= A_1 \sin \rho_1 t + A_2 \sin \rho_2 t \\ Y_c &= A_1 B_1 \sin \rho_1 t + A_2 B_2 \sin \rho_2 t \end{aligned} \right\} \dots\dots(15)$$

The equations of energy become:

$$\begin{aligned}
 V_s &= \int^{Y_1} K_s Y_s dY_s = \int^t K_s Y_s \dot{Y}_s dt \\
 &= 1/2 K_s (A_1 \sin \rho_1 t + A_2 \sin \rho_2 t)^2 \\
 V_f &= \int^t K_f (Y_c - Y_s) (\dot{Y}_c - \dot{Y}_s) dt \\
 &= 1/2 K_f [A_1 (B_1 - 1) \sin \rho_1 t \\
 &\quad + A_2 (B_2 - 1) \sin \rho_2 t]^2
 \end{aligned} \left. \right\} \dots\dots(16)$$

In the case of a very rigid berth, which offers a large resistance, the deflection  $Y_s$  will be very small and, consequently, its ability for energy absorption will be very poor, and can, therefore, be neglected. In this case all the portion of energy consumed in the swaying motion of the ship should be absorbed by the fenders.

*Notations*

- $I_{1-1}$  = polar moment of inertia about the longitudinal axis (1-1) passing through the C.G.
  - $I_{2-2}$  = polar moment of inertia about the vertical axis (2-2) passing through the C.G.
  - $M_1$  = the effective mass of the structure.
  - $M_2$  = the virtual mass of the ship while swaying.
  - $P$  = the ship acting load.
  - $H, H_1$  = the vertical distances between the C.G. and the point of contact and the meta-center respectively.
  - $r$  = the distance from the C.G. to the point of contact.
  - $w$  = the ship's displacement weight.
  - $\gamma$  = the angle that the velocity vector makes with the arm  $r$  at time of the first contact.
- } \dots\dots(17)

$K_x, K_y$ =structure stiffness in  $X$  and  $Y$  direction.

$\mu_x, \mu_y$ =structure damping coefficients in  $X$  and  $Y$  direction.

$X_s, X_y$ =the displacement of the structure in  $X$  and  $Y$  direction.

$$A_1 = V_0/\rho_1(B_1 - B_2)$$

$$A_2 = -V_0/\rho_2(B_1 - B_2)$$

$$\rho_{1,2}^2 = (a+b)/2 \mp \sqrt{[(a+b)/2]^2 + bc}$$

$$B_1 = b/(\rho_1^2 - a)$$

$$B_2 = b/(\rho_2^2 - a)$$

$$a = (K_s + K_f)/M_1$$

$$b = K_f/M_1$$

$$c = K_f/M_2$$

### 3. SELECTION OF THE PARAMETERS FOR SOLUTIONS OF THE DYNAMIC EQUATIONS

The dynamic equations of motion presented in section 2 contain the following parameters;

for the ship,  $V_0, M_2, I_{1-1}, I_{2-2}, H_1,$

for the structure,  $M_1, K_s,$

for the fender,  $(P, D)$

and in practical design, the ship's displacement weight ( $W$ ) is, generally, the only value given with the information for the marine structure to be constructed.

This section includes equations, tables, and graphs to help in selecting or computing the unknown parameters for solutions of the dynamic equations.

#### (1) Approach Velocity, $V_0$

From eq. (1) the impact energy is proportional to the square of the approach velocity. Thus, the energy level will increase considerably if the velocity is only slightly increased. In the selection of this velocity for design, many factors should be considered, such as:

##### 1) Method of docking

A ship approaching the berth under the control of tugboats usually berths with less velocity

than one approaching under its own power.

##### 2) Berthing conditions

In the case where the berth is exposed to wind, waves, currents, etc., it is more difficult to control the ship velocity than in a sheltered berth and the velocity may become large. However, for extremely high wind velocities in the order of 100 to 120 mph that occur during short periods, it is advisable to require ships to temporarily anchor away from the berth in order to avoid being damaged<sup>11)</sup>.

##### 3) Ship size

Larger ships are always berthed with great care and with the assistance of tugboats. It is generally assumed that the larger the ship, the smaller will be the velocity with which the ship will contact the fender system<sup>5)</sup>.

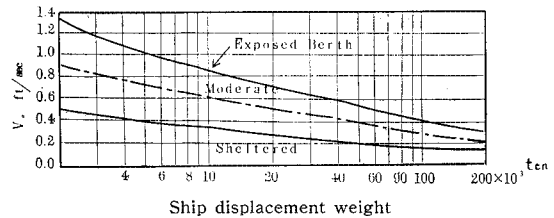


Fig. 2 Berthing velocity normal to dock vs. Ship displacement weight (after Lee).

T. Lee presented the curves shown in Fig. 2 from which the berthing velocity may be selected for design. Under various conditions of berthing, Vasco Costa<sup>5)</sup> recommended Table 1 as a guide for the selection of velocity.

Before proceeding to the selection of other parameters, some relations concerning the ship characteristics will be discussed. For example, a tanker of length  $L$ , draft  $d$  and beam breadth  $B$ , Fig. 1, will have the following empirical relations:

$$\left. \begin{aligned} W &= c_B \rho L B d \\ c_B &= 0.75 \text{ to } 0.80 \div 0.78 \end{aligned} \right\}$$

Table 1 Approach velocity of berthing ships

| Wind and swell          | Approach conditions | Displacement of the ship |                  |                 |
|-------------------------|---------------------|--------------------------|------------------|-----------------|
|                         |                     | (ft/sec)                 |                  |                 |
|                         |                     | Up to 3,000 ton          | Up to 10,000 ton | Over 30,000 ton |
| Strong wind and swell   | Difficult           | 2.5                      | 2.0              | 1.5             |
| Strong wind and swell   | Favourable          | 2.0                      | 1.5              | 1.0             |
| Moderate wind and swell | Moderate            | 1.5                      | 1.0              | 0.8             |
| Protected               | Difficult           | 1.0                      | 0.8              | 0.6             |
| Protected               | Favourable          | 0.8                      | 0.6              | 0.4             |

(after V. Costa)

$$\left. \begin{aligned}
 D/d &= \text{total depth/draft} = 1.33^{15)} \\
 L/D &= 13.75 \\
 L/d &= 18.25 \\
 OG &= d - 0.52D = 0.31d \\
 k &= \text{radius of gyration about vertical axis through } G = 0.2L^{15)} \\
 k_x &= \text{radius of gyration about longitudinal axis through } G = n'B \\
 n' &= 0.37 \text{ to } 0.47 \cong 0.42
 \end{aligned} \right\} \dots (18)$$

(2) Derivation of Added Mass Equations for Berthing in Shallow Water

1) Added mass in horizontal motion,  $M_2$

It is well known that when a ship moves from deep to shallow water, as in the case when berthing, the added virtual mass is increased due to the presence of restricting boundaries. Koch<sup>12)</sup> investigated the effects of shallow water on added virtual weight for both vertical and horizontal vibration. The measurements were made for a block having a half-beam  $b$  and a draft  $d$ . The results of the experiments are shown in Fig. 3. To apply the Koch results on hull shape sections, it is suggested that the added weight to any section of the ship, calculated for deep water for this particular section shape, should be increased by the ratio of the added weights in shallow and deep water for a rectangular section of the correct beam-draft ratio and depth of water.

Furthermore, on the basis that many modern tankers have very similar hull shapes, sections

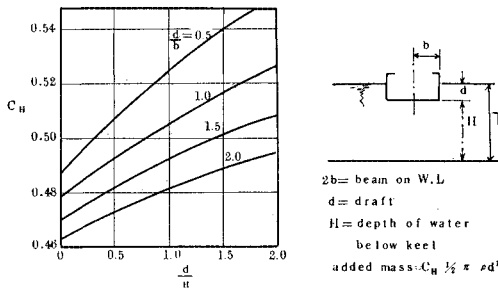


Fig. 3 Effect of shallow water on added mass in horizontal vibration, Curves of  $C_H$  for rectangular section (after Koch).

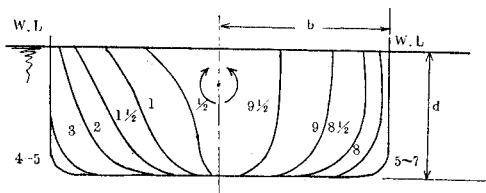


Fig. 4 Actual sections of ship (after Kumai).

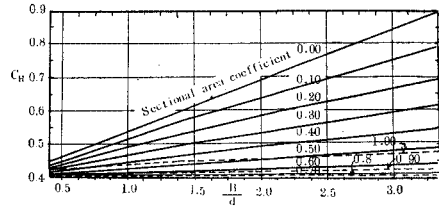


Fig. 5 Values of added mass coefficient  $C_H$  for horizontal motion in deep water.

for typical tankers, Fig. 4<sup>12)</sup>, are considered in the analysis hereafter.

With the help of the curves of Fig. 5 and these sections, the distribution of the added mass along the ship length may be obtained (step 6 in Table 2, and curve a Fig. 7). Considering the Koch results for rectangular sections, and the procedure above, the added mass of actual hull shape sections, where the ratio of water depth  $T$  to draft  $d$  is 2.0, can be evaluated (steps 7 to 10, Table 2). The results are shown by curve  $b$  of Fig. 7).

However, the water depth considered by Koch was deeper than that required for berthing. The experimental results obtained by Marwood and Johnson, Fig. 6 are of considerable help in this field<sup>12)</sup>. This is bearing on the fact that the percentage increase in  $C_H$  in shallow water, where  $T/d=2.0$ , than that in deep water for the ship mid-sections (4-7), computed on the basis

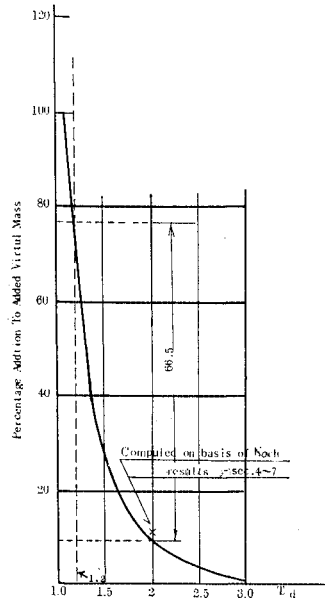


Fig. 6 Effect of shallow water on added mass —(Marwood & Johnson).

Table 2 Evaluation of added mass in shallow water

| Section No. | →                                                          | 0   | $\frac{1}{2}$ | 1     | $1\frac{1}{2}$ | 2     | 3     | 4     | 5     | 6     | 7     | 8     | $8\frac{1}{2}$ | 9     | $9\frac{1}{2}$ | 10  |
|-------------|------------------------------------------------------------|-----|---------------|-------|----------------|-------|-------|-------|-------|-------|-------|-------|----------------|-------|----------------|-----|
| 1           | $b=1/2$ beam on W.L.                                       | 0.0 | 12.0          | 18.5  | 23.0           | 26.0  | 27.5  | 27.5  | 27.5  | 27.5  | 27.5  | 26.5  | 24.5           | 19.0  | 10.0           | 0.0 |
| 2           | $A=b \times d$ ( $d=21$ )                                  | 0.0 | 441           | 388.5 | 483            | 546   | 577.5 | 577.5 | 577.5 | 577.5 | 577.5 | 556.5 | 514.5          | 399   | 210            | 0.0 |
| 3           | $S=$ Actual area                                           | 0.0 | 111           | 250.3 | 339.5          | 441.5 | 558.5 | 574.4 | 574.4 | 573.8 | 573.8 | 536   | 573.13         | 365.5 | 195            | 0.0 |
| 4           | $\sigma=$ Area. coeff. $S/A$                               | 1.0 | 0.252         | 0.644 | 0.703          | 0.809 | 0.967 | 0.995 | 0.995 | 0.994 | 0.994 | 0.963 | 0.929          | 0.916 | 0.929          | 1.0 |
| 5           | $2b/d$                                                     | 0.0 | 1.143         | 1.762 | 2.190          | 2.476 | 2.619 | 2.619 | 2.619 | 2.619 | 2.619 | 2.524 | 2.333          | 1.810 | 0.952          | 0.0 |
| 6           | $C_{H_0}$ (Deep water)<br>Fig. 5                           | 0.0 | 0.49          | 0.42  | 0.42           | 0.405 | 0.44  | 0.46  | 0.46  | 0.46  | 0.46  | 0.44  | 0.42           | 0.415 | 0.41           | 0.0 |
| 7           | $C_{H'}$ (Deep water)<br>$\sigma=1$                        | 0.0 | 0.445         | 0.45  | 0.46           | 0.465 | 0.465 | 0.465 | 0.465 | 0.465 | 0.465 | 0.465 | 0.46           | 0.45  | 0.44           | 0.0 |
| 8           | $d/b$                                                      | 0.0 | 1.75          | 1.135 | 0.913          | 0.808 | 0.764 | 0.764 | 0.764 | 0.764 | 0.764 | 0.792 | 0.857          | 1.105 | 2.10           | 0.0 |
| 9           | $C_{H''}$ (Shallow W.)<br>$T/d=2.0$ $\sigma=1$<br>Fig. 3   | 0.0 | 0.488         | 0.501 | 0.510          | 0.512 | 0.516 | 0.516 | 0.516 | 0.516 | 0.516 | 0.513 | 0.511          | 0.502 | 0.48           | 0.0 |
| 10          | $C_H$ (Shallow W.)<br>$C_H=C_{H_0} \frac{C_{H''}}{C_{H'}}$ | 0.0 | 0.537         | 0.468 | 0.466          | 0.446 | 0.488 | 0.510 | 0.510 | 0.510 | 0.510 | 0.485 | 0.467          | 0.463 | 0.477          | 0.0 |
| 11          | $C_H$ for shallow W.<br>$T/d=1.2$                          | 0.0 | 0.886         | 0.772 | 0.769          | 0.736 | 0.805 | 0.840 | 0.840 | 0.840 | 0.840 | 0.80  | 0.771          | 0.764 | 0.738          | 0.0 |

of the Koch results, showed a close agreement with Marwood and Johnston's experimental results, as indicated in Fig. 6.

Taking into account the results shown in Fig. 6, the derived values of the added mass coefficients in step 10 are re-calculated for a water depth and draft ratio of 1.2 (step 11, Table 2 and curve c, Fig. 7).

By integrating along the length and substituting for  $d=B/2.61$  from Table 2, the following equation, for the added mass in horizontal vibration, was derived;

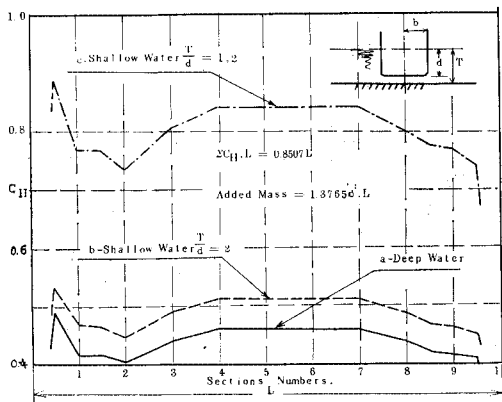


Fig. 7 Distribution of added mass along length.

$$m' = \frac{1}{2} \rho d B L \tag{10}$$

The virtual mass becomes

$$M_2 = m + m' \tag{20}$$

and the virtual moment of inertia  $I_{2-2}$ , in yawing motion will be<sup>(2),5)</sup>

$$I_{2-2} = M_2 k^2 \tag{21}$$

2) Checking the derived formula

Taking into account both model and prototype experiments, Vasco Costa<sup>5)</sup> presented the following equation for estimating the virtual mass of a berthing ship;

$$M_v = M + m' = m(1 + 2d/B) \tag{22}$$

Shu T'ien Li<sup>11)</sup> also presented the following equation;

$$M_v = m(1 + \pi B/(16D)) \tag{23}$$

The virtual mass for different tankers, using the three equations, was calculated, Table 3. It can be seen that the derived equations yield results which are about 5% more than the Shu T'ien Li equation and about 5% less than the Vasco Costa equation.

3) Added mass of inertia in rolling motion

The added mass moment of inertia coefficients depend upon the sectional shapes and the ratio of beam to draft; the same parameters which

Table 3

| D/W     | Displ. W. | $\frac{L}{m}$ | B    | d    | I       | II      | III     | $\frac{III}{I}$ |
|---------|-----------|---------------|------|------|---------|---------|---------|-----------------|
| Tankers | ton       | m             | m    | m    | ton     | ton     | ton     | %               |
| 10 000  | 13 300    | 140           | 17.2 | 7.9  | 25 500  | 19 000  | 24 700  | 97.0            |
| 20 000  | 26 700    | 178           | 22.4 | 9.5  | 48 000  | 39 000  | 47 750  | 99.9            |
| 30 000  | 40 000    | 200           | 25.8 | 10.3 | 72 000  | 59 600  | 68 200  | 95.0            |
| 50 000  | 66 600    | 230           | 32   | 11.4 | 114 000 | 103 000 | 105 700 | 92.5            |
| 85 000  | 113 000   | 260           | 38.1 | 14.0 | 196 000 | 173 000 | 180 000 | 92.0            |
| 100 000 | 133 000   | 285           | 41.2 | 14.6 | 223 000 | 206 700 | 213 000 | 95.0            |

I=Vasc Costa Formula  
 II=Shu T'ien Li Formula  
 III=The New Formula

average: 95%

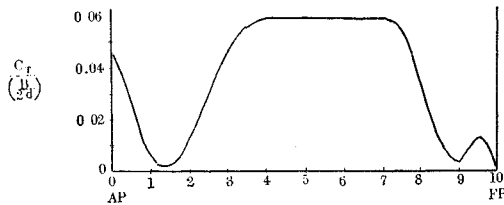


Fig. 8 Distribution of added virtual weight along length in torsional vibration (after Kumai).

effect  $C_H$ . Also, these coefficients depend on the location of the center of rotation. Model experiments were carried out by Kumai on prismatic models having sections corresponding to those of a tanker<sup>12)</sup>. Applying the experimental results on the actual sections of a tanker ship, Fig. 4, Kumai obtained the distribution of the added mass moment of inertia along a typical tanker hull in the loaded condition, Fig. 8. By integrating along the length, Kumai derived the following expression;

$$\Delta I_0 = 0.00531(1 + 0.365d/d_f)B^4L \quad (\text{ton}\cdot\text{m}^2) \quad \dots\dots(24)$$

For a fully loaded tanker ( $d=d_f$ ), the above expression becomes;

$$\Delta I_0 = 0.00725B^4L \quad (\text{ton}\cdot\text{m}^2) \quad \dots\dots(25)$$

Eq. (24) represents the added mass moment of inertia in deep water, but, as was discussed previously, berthing always takes place in shallow waters. Therefore, the effect of shallow water on the inertial moment has to be considered.

Matsuura and Kawakami<sup>13)</sup> performed numerical computations, applying the finite element method, on the effect of the restricted water on the inertial coefficients,  $C_T$ . Rectangular sections having a ratio of half-beam to draft of 1.0 and two locations of center of rotation,  $y_0/d=0.0$  and 1.5, were investigated, Fig. 9.

To apply the results shown in Fig. 9 to the case of a fully loaded ship, the following corrections are necessary; a) first, since we are interested in the moment of inertia ( $I_{1-1}$ ) about the center of gravity of the ship where  $y_0/d=0.31$ , eq. (18), the effect of shallow water on the cen-

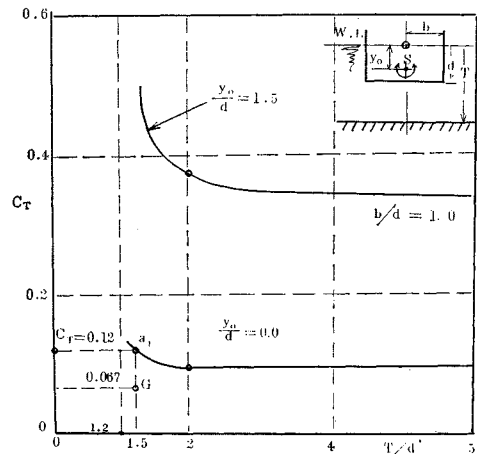


Fig. 9 Effect of shallow water on added mass moment of inertia in rolling (after Matsuura & Kawakami).

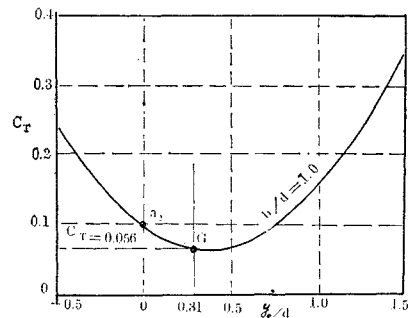


Fig. 10 Variation of  $C_T$  with respect to center of rotation for  $b/d=1.0$  (after Matsuura & Kawakami).



ter of rotation becomes important. This is obtained by comparing the inertial coefficients,  $C_T$ , at point  $a_1$  where  $T/d=1.2$ , Fig. 9, with point  $a_2$  in Fig. 10. That is,

$$C_{Ta_1}/C_{Ta_2}=0.12/0.1=1.2$$

From which the value of  $C_T$  at  $y_0/d=0.31$  and  $T/d=1.2$ , namely  $C_{TG}$ , will approximately be equal to

$$C_{TG}=1.2(0.056)=0.067 \quad \dots\dots(26)$$

b) The second correction is obtained from the consideration of three dimensional motion. The correction factors from 2 to 3 dimensional motion can be obtained from Fig. 11<sup>14)</sup>. If  $L/d=18.25$ , eq. (18), the correction factor corresponding to pure rolling, ( $n=0$ ), is equal to 0.96. Multiplying eq. (26) by this value yields;

$$C_{TG}=0.067(0.96)=0.064 \quad \dots\dots(27)$$

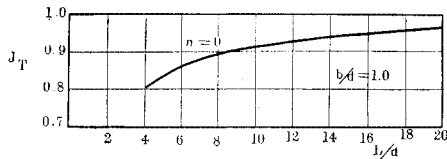


Fig. 11 Taylor correction factor from 2 to 3 dimensional motion.

c) The third correction is obtained from the effect of actual ship hull sections. A comparison was made with sections 4 to 7, Fig. 8, having  $C_T$  in deep water equal to 0.06, and the rectangular-shaped sections where  $C_T$  in shallow water was derived, eq. (27). From Table 2 the area coefficient ( $\sigma$ ) of these sections is equal to 0.996 or about 1.0, giving a very slight effect due to the round edges of these particular sections. The other sections have already been considered by the use of the equation derived by Kumai,

eq. (24). Hence, for deduction, the  $C_T$  values of ship sections in shallow water (values included in Fig. 8) can be multiplied by the ratio 0.064/0.06, which denotes the  $C_T$  value in shallow water as compared to deep water for sections 4 to 7. This will lead, finally, to multiplying eq. (25) with the above ratio for obtaining the added mass moment of inertia, as follows, in shallow water;

$$\Delta I_0=0.00774B^4L \quad (\text{ton}\cdot\text{m}^2) \quad \dots\dots(28)$$

The polar moment of inertia,  $I_0$ , about a longitudinal axis passing through  $G$  is equal to

$$I_0=m(k_x)^2$$

and substituting from eq. (18) results

$$I_0=0.78\rho LBd(0.42B)^2$$

Letting  $d=B/2.62$  from Table 2, step 5,  $\rho=1.03 \text{ ton/m}^3$

$$I_0=0.0541B^4L \quad (\text{ton}\cdot\text{m}^2)$$

$$\Delta I_0/I_0=(0.00774B^4L)/(0.0541B^4L)=0.143$$

$$\dots\dots(29)$$

This ratio is in close agreement with the ratio of 0.15 given by Prof. Hayashi<sup>15)</sup>. The virtual moment of inertia  $I_{1-1}$  becomes

$$I_{1-1}=1.143m(k_x)^2=0.202B^2m \quad (\text{ton}\cdot\text{m}^2)$$

$$\text{or } I_{1-1}=I_0+\Delta I_0=0.0618B^4L \quad (\text{ton}\cdot\text{m}^2)$$

$$\dots\dots(30)$$

4)  $H_1$  or  $\overline{GM}$ , which denotes the vertical distance between the ship's center of gravity,  $G$ , and its metacentre,  $M$ , Fig. 1, can be calculated from the following equation<sup>15)</sup>;

$$B=L/C_1+\overline{GM}(d/D)C_2 \quad \dots\dots(31)$$

where  $C_1$  and  $C_2$  are constants having the following values for oil tankers (where  $\overline{KG}/D=0.52$ );

$$C_1=12.5 \text{ (U-shape)} \sim 13.2 \text{ (V-shape)}$$

$$C_2=5.7$$

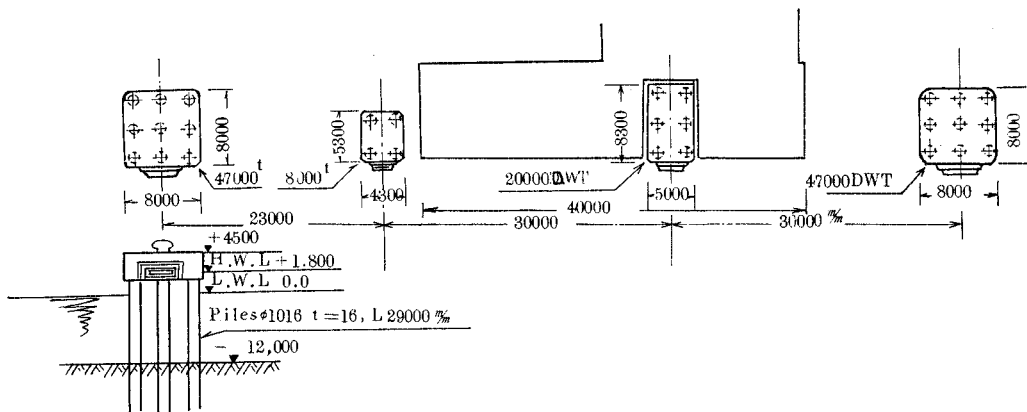


Fig. 12 Mitsubishi Shoji Oil Berth.

5) Effective mass,  $M_1$ , of the structure

For determining the value of  $M_1$  that should be substituted in the motion equations, the authors investigated some existing berths in Kobe harbor.

One is an oil berth belonging to the Mitsubishi Shoji Co. which consists of four dolphins of different sizes and a platform, Fig. 12, located back from the berth line. The berth is provided with V-type rubber fenders. The berth was designed to accommodate tankers varying in size (8 000, 20 000 and 47 000 DWT) under the control of tugboats.

a) The 47 000 DWT berths against two dolphins which have an effective weight equal to

$$\begin{aligned} & \text{cap} + \text{effective piles weight} \\ & = 2(160 + 180) = 680 \text{ tans.} \end{aligned}$$

b) The 20 000 DWT should use two dolphins which have an effective weight equal to

$$2(100 + 120) = 440 \text{ tons.}$$

c) The 8 000 DWT should berth against two dolphins which have an effective weight equal to

$$2(60 + 80) = 280 \text{ tons.}$$

The displacement weights of the above ships are approximately (1.3 W) or 61 000, 26 000 and 10 400 tons, respectively. The virtual masses ( $M_2$ ) will be equal to 104 000, 48 000 and 25 000 tons, respectively, Table 1 and the ratio  $M_1/M_2$  will be equal to  $680/104\ 000 = 0.007$ ,  $440/48\ 000 = 0.009$ , and  $280/25\ 000 = 0.011$ .

$$M_1/M_2 = 0.01 \quad \dots\dots(32)$$

Thus for the first design approximation, we can assume that  $M_1$  will be as much as 1% of the virtual mass,  $M_2$ , of the approaching ship. If, at the end of the calculations, the difference between the derived value of  $M_1$  and the assumed value is great, the calculations can be repeated using the derived value for  $M_1$ .

## 6) Structure and fender resistance

As discussed previously for the design of marine structures, the function of the structure should be known in advance in addition to the ship displacement weight. In the selection of the resistance ( $K_S$ ) of the structure, the structure functions, whether rigid or flexible, should be considered. If the berth carries heavy loads (heavy, delicate equipment carried on the deck, cranes, power station, etc.), there is no choice; deflection must be limited. The construction should be rigid and provided with elastic fenders to absorb the ship's kinetic energy. On the other hand, if deflection is allowed, the berth can be flexible. A pile dolphin is a good example for this type.

## 4. SOLUTIONS OF THE DYNAMIC EQUATIONS BY NUMERICAL INTEGRATION

The differential equations of motion of the ship and the berthing structure are in the form of:

$$\left. \begin{array}{l} \text{Structure} \quad \ddot{X}_s = f(X_s, P(X_s, X_c), \dot{X}_s) \\ \text{Ship} \\ \quad \text{i) roll} \quad \ddot{\phi} = G(\phi, P(X_s, X_c), \dot{\phi}_1) \\ \quad \text{ii) yaw} \quad \ddot{\theta} = G_1(\theta, P(X_s, X_c), \dot{\theta}) \\ \quad \text{iii) sway} \quad \ddot{X}_c = G_2(X_c, \dot{\theta}, \dot{\phi}, P(X_s, X_c), \\ \quad \quad \quad \quad (X_c - X_s)) \end{array} \right\} \dots\dots(33)$$

(These notations are explained in section 2.)

In eq. (33) the first differential terms represent the damping effect which is generally neglected. Solutions of eq. (33) are quite difficult to be carried out analytically, especially in the case where fenders (such as rubber) that have non-linear spring constants are used.

A numerical solution implies the determination of the displacement and velocity of a system as a function of time. These displacements and velocities are obtained in a step-by-step integration procedure, starting with given initial conditions. There are many different methods of numerical integration from which two methods, the Newmark  $\beta$  method<sup>(16)</sup> and the Runge-Kutta-Gill method<sup>(17)</sup>, will be explained.

## (1) Time Interval Effect on the Two Numerical Integration Methods

Tests have been conducted to study the effect of the time interval on the accuracy of the two methods. In these tests, fenders with linear spring constants were used, for which the exact solution of the equation of motion is obtained by using eq. (15). Through the comparison of results which are included in Table 4 and Fig. 13, the following conclusions could be made:

- 1) The error involved in fender absorbed energy,  $V_F$ , is relatively small compared to the energy  $V_s$  absorbed by the structure.
- 2) The percentage of error involved in the  $V_s$  values is nearly twice that of the structure maximum deflection,  $X_1$ , i.e.  $\Delta V_s\% = 2\Delta X_1\%$ .
- 3) For the same time interval the error incurred using the Runge-Kutta-Gill method is greater than that involved in the Newmark  $\beta$  method. The difference also increases as the time interval is increased.

Table 4 Convergence of error with respect to time interval variation

| $K_1$<br>ton·cm | Berthing data   |                                   |                 | Max<br>value of | Exact<br>solution | Method<br>name | $\Delta T=0.01$ |            | 0.0075   |            | 0.005    |            | 0.0025   |            |          |            |
|-----------------|-----------------|-----------------------------------|-----------------|-----------------|-------------------|----------------|-----------------|------------|----------|------------|----------|------------|----------|------------|----------|------------|
|                 | $K_2$<br>ton·cm | $M_1$<br>ton·sec <sup>2</sup> ·cm | $M_2$<br>cm·sec |                 |                   |                | Absolute        | ERROR<br>% | Absolute | ERROR<br>% | Absolute | ERROR<br>% | Absolute | ERROR<br>% | Absolute | ERROR<br>% |
|                 |                 |                                   |                 |                 |                   |                |                 |            |          |            |          |            |          |            |          |            |
| 800             | 60              | 0.3                               | 30              | 20              | 1.049             | Newmark        | 1.299           | 23.8       | 1.190    | 13.4       | 1.67     | 10.6       | 1.091    | 4.0        |          |            |
|                 |                 |                                   |                 |                 |                   | Rung-Kutta     | **              | **         | 6.710    | 539        | 2.167    | 106        | 1.198    | 14.2       |          |            |
|                 |                 |                                   |                 |                 |                   | Newmark        | 674             | 53         | 569      | 29         | 538      | 22         | 476      | 8.2        |          |            |
|                 |                 |                                   |                 |                 |                   | Rung-Kutta     | **              | **         | 18 009   | ~          | 1 879    | 327        | 575      | 30.7       |          |            |
|                 |                 |                                   |                 |                 |                   | Newmark        | 5 823           | 4.5        | 5 751    | 3.2        | 5 672    | 1.8        | 5 604    | 0.6        |          |            |
|                 |                 |                                   |                 |                 |                   | Rung-Kutta     | **              | **         | 10 778   | **         | 6 335    | 14         | 5 670    | 1.8        |          |            |
| 200             | 30              | 0.3                               | 30              | 20              | 2.867             | Newmark        | 3.076           | 7.3        | 3.027    | 5.3        | 2.959    | 3.41       | 2.912    | 1.6        |          |            |
|                 |                 |                                   |                 |                 |                   | Rung-Kutta     | 3.964           | 38.3       | 3.410    | 18.9       | 3.111    | 8.5        | 2.952    | 3.0        |          |            |
|                 |                 |                                   |                 |                 |                   | Newmark        | 946             | 15.2       | 916      | 11.6       | 875      | 6.5        | 848      | 3.3        |          |            |
|                 |                 |                                   |                 |                 |                   | Rung-Kutta     | 1 571           | 91         | 1 163    | 41.6       | 968      | 17.9       | 871      | 6.8        |          |            |
|                 |                 |                                   |                 |                 |                   | Newmark        | 5 397           | 2.5        | 5 364    | 1.9        | 5 321    | 1.14       | 5 290    | 0.55       |          |            |
|                 |                 |                                   |                 |                 |                   | Rung-Kutta     | 6 043           | 14.8       | 5 630    | 7.0        | 5 420    | 3.0        | 5 315    | 1.0        |          |            |
| 800             | 60              | 4.5                               | 90              | 15              | 1.376             | Newmark        | 1.419           | 3.1        | 1.406    | 2.2        | 1.395    | 1.4        | 1.385    | 0.6        |          |            |
|                 |                 |                                   |                 |                 |                   | Rung-Kutta     | 1.462           | 6.3        | 1.434    | 4.2        | 1.410    | 2.5        | 1.392    | 1.16       |          |            |
|                 |                 |                                   |                 |                 |                   | Newmark        | 805             | 6.3        | 791      | 4.5        | 778      | 2.7        | 767      | 1.3        |          |            |
|                 |                 |                                   |                 |                 |                   | Rung-Kutta     | 855             | 12.9       | 823      | 8.7        | 795      | 5.02       | 775      | 2.37       |          |            |
|                 |                 |                                   |                 |                 |                   | Newmark        | 9 551           | 0.78       | 9 531    | 0.5        | 9 512    | 0.3        | 9 495    | 0.15       |          |            |
|                 |                 |                                   |                 |                 |                   | Rung-Kutta     | 9 589           | 1.16       | 9 552    | 0.77       | 9 522    | 0.45       | 9 498    | 0.2        |          |            |

\*\* derived results are meaningless.

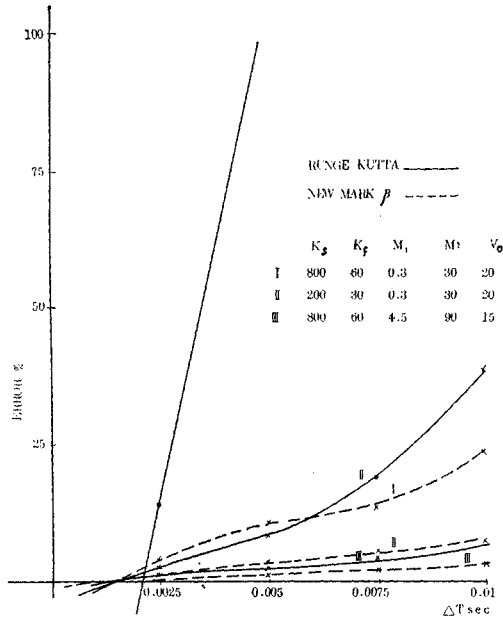


Fig. 13 Convergence of error with respect to time interval.

(2) Selection of a Suitable Time Interval

Through many investigations carried out by the authors, Fig. 4, a formula linking the time

interval variation, the berthing data, and the error involved in the maximum deflection of the berthing structure was developed.

The curves shown in Fig. 15 were plotted from Fig. 14 for an error equal to 2% of the structure maximum deflection. This gives 2% error in the structure maximum reaction ( $K_s X_s$ ) and nearly 4% in the structure's stored energy. In this figure the  $x$ -axis represents the berthing data, which is the factor  $N$ , and the  $y$ -axis represents the time interval  $\Delta t$ . The factor  $N$  is a function of the ship's virtual mass, the structure's effective mass, the structure and fender spring constants, and the ship's approaching velocity according to the following equation;

$$N = (M_1/M_2 A_1)(100) \text{ (cm)} \quad \dots\dots(34)$$

where  $A_1$  is obtained from eq. (17).

From Fig. 15 the relation between  $N$  and the time interval  $\Delta t$  for an error of 2% in  $\Delta X_1$  is given by:

i) The Newmark  $\beta$  method ( $\beta=1/4$ )  
 $\Delta t = 0.00067N + 0.0012 \text{ (sec).} \quad \dots\dots(35)$

$$N \leq 3.73$$

$$\Delta t = 0.00015N^3 - 0.0029N^2 + 0.018N - 0.0313 \text{ (sec)} \quad \dots\dots(36)$$

$$N \geq 3.73$$

ii) The Runge-Kutta-Gill method

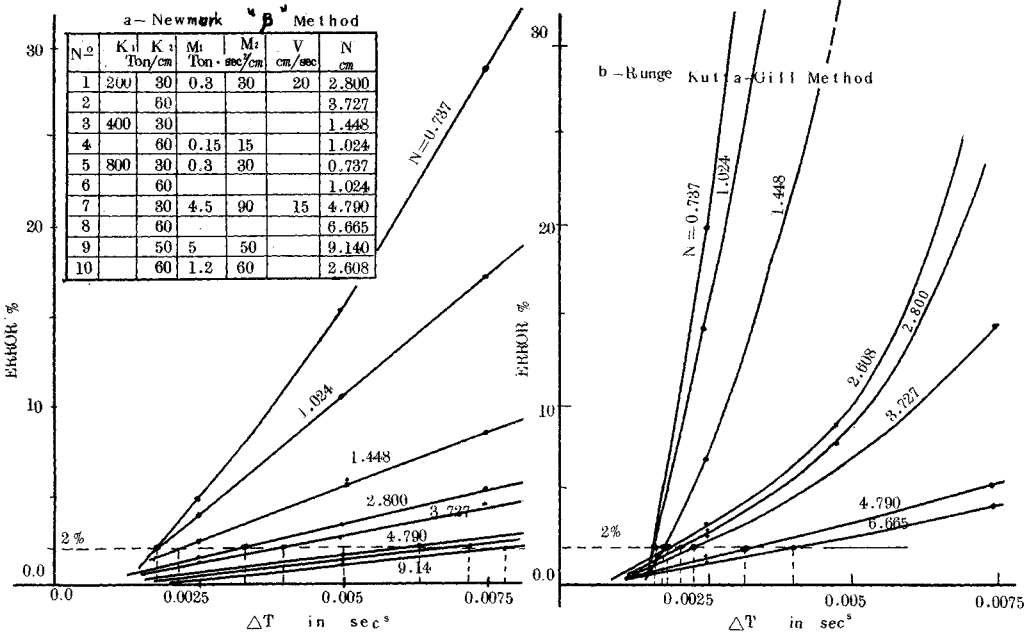


Fig. 14 Effect of time interval on the berth structure max deflection for different cases of berthing.

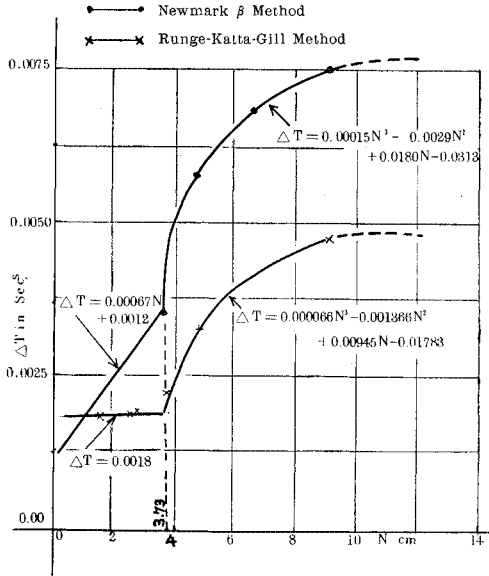


Fig. 15  $\Delta T$ , vs.  $N$  for 2% error in berth structure max deflection.

$\Delta t = 0.0018$  (sec) .....(37)

$N \leq 3.73$

$\Delta t = 0.000066N^3 - 0.00137N^2 + 0.0095N - 0.0178$  (sec) .....(38)

$N \geq 3.73$

(3) Application to the Non-linear Spring Constant Fenders

Both rubber and retractable fenders possess non-linear relations between the load and the displacement. To apply the preceding equations for selecting the time interval for structures provided with these type of fenders, the load is considered to be applied in small increments associated with the time interval. The procedure for calculation is as follows:

- 1) The spring constant ( $K_s$ ) of the fender corresponding to zero displacement is taken from the given load-displacement relationship.
- 2) The factor  $N$  can be calculated and, consequently, the time interval from eqs. (35), (36) or eqs. (37), (38).
- 3) Substituting in the equations of motion, the displacement of the fender at the end of the interval can be obtained.
- 4) The spring constant corresponding to this displacement can be calculated as indicated in step 1).
- 5) Repeating steps 2), 3), and 4) until the allowable fender displacement is reached.

5. APPLICATION

(1) A Case of General Berthing and Fenders of Non-linear Spring Constant

Solved Example

a) Data Given;  
 A tanker ship of displacement weight  $W = 40\,000$  ton  
 Approaching velocity  $V_0 = 15$  cm/sec  
 Ship characteristics are;  
 Length = 200 m Breadth = 25.8 m  
 Draft = 10.8 m  
 Berthing data;  
 $r = 80$  m  $H = 3.0$  m  $\gamma = 50^\circ$   $\alpha = 20^\circ$   
 Assuming, for the first trial, the fender system data as;  
 $K_s = 15$  ton/cm Fender = 2 pieces of type I, Fig. 17.

b) By applying the formulas included in section 3, the following data was computed;  
 $M_2 = 70.69$  ton·sec<sup>2</sup>/cm

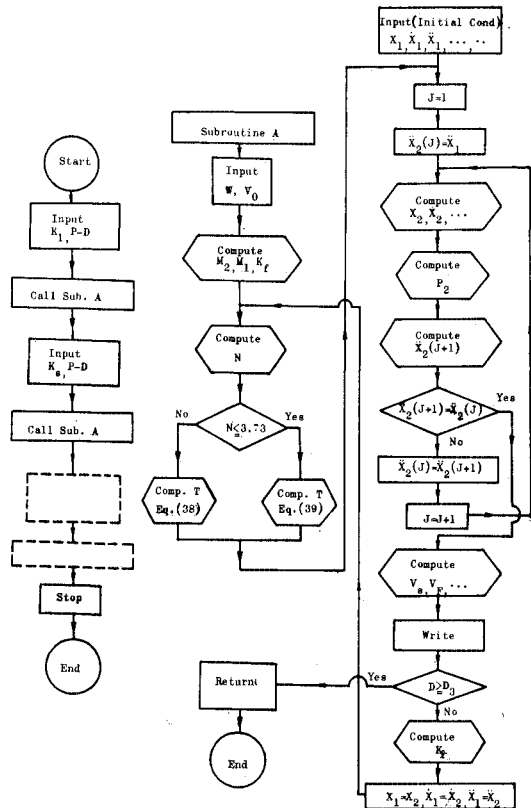


Fig. 16 Flow chart for design procedure by using newmark "β" method.

Table 5

| Case No. | Mode of berthing                 | $\gamma^\circ$ | $r$<br>m | $H$<br>m | $K_s$<br>ton/cm | Fender Fig. 17                  | Effective energy $E_e$ | $C = \frac{E_e}{E_0}$<br>% | $\dot{\theta}$<br>sec <sup>-1</sup> | $\dot{\phi}$<br>sec <sup>-1</sup> |
|----------|----------------------------------|----------------|----------|----------|-----------------|---------------------------------|------------------------|----------------------------|-------------------------------------|-----------------------------------|
| 1        | General berthing                 | 50             | 80       | 3        | 15              | Type I                          | 41.79                  | 52.6                       | $0.1112 \times 10^{-2}$             | $0.151 \times 10^{-2}$            |
| 2        | No-rolling                       | "              | "        | 0        | 15              | "                               | 42.09                  | 53.44                      |                                     |                                   |
| 3        | Fender of linear spring constant | 90             | 60       | 0        | 25              | 6.25                            | 36.70                  | 56.5                       |                                     |                                   |
|          |                                  |                |          |          |                 | $K_T = 500 \text{ ton/m} = C_T$ |                        | 37.60                      | 57.7                                | Tables 3 and 4 refer. 4)          |

\*  $K_x = K_y$

\*\* The fender stiffness used in these cases is chosen by trials to give  $V_c = 0.0$  at max. sway.

\*\*\*  $M_2 = 130 \text{ ton} \cdot \text{sec}^2 / \text{cm}$ ,  $V_0 = 10 \text{ cm/sec}$

\*\*\*\*  $K_T =$  the compound stiffness of the fender system  $= K_s K_f / (K_s + K_f)$

$M_1 = 0.7 \text{ ton} \cdot \text{sec}^2 / \text{cm}$

$H_1 = \bar{G}\bar{M} = 2.27 \text{ m}$

$I_{1-1} = 54 \times 10^6 \text{ ton} \cdot \text{sec}^2 \cdot \text{cm}^3$

$I_{2-2} = 113 \times 10^7 \text{ ton} \cdot \text{sec}^2 \cdot \text{cm}^3$

c) For numerical integration, Newmark  $\beta$  method with  $\beta = 1/4$  was used. Besides, equations (35) and (36) were applied for selecting the time interval. Calculations were carried out by the digital computer, the flow of computations is shown by the block diagram Fig. 16. Results is included in Table 5.

(2) Besides, for comparing the presented method with other investigators methods, two other examples were tried, Table 5.

6. COMMENTS ON THE RESULTS

(1) Verification of the Developed Method of Analysis

To verify the assumptions presented in establishing the dynamic equations included in section 2, conservation of energy before and after collision is checked from the deduced results.

1) Conservation of the kinetic energy

From Table 5 we have at  $V_c = 0.09 \div 0.0$

i) Part of the ship's kinetic energy transmitted to:

Fender system = Effective energy

$E_e = 41.79 \text{ (ton/m)}$

ii) Part of energy induced by the system vibration:

Ship

$$E_{sh} = \frac{1}{2} M_2 (\dot{X}_G^2 + \dot{Y}_G^2) + \frac{1}{2} I_{2-2} \dot{\theta}^2 + \frac{1}{2} I_{1-1} \dot{\phi}^2$$

at  $V_c = 0.0$  this eq. yields to;

$$E_{sh} = \frac{1}{2} M_2 (r \cdot \dot{\theta} + H \cdot \dot{\phi})^2 + \frac{1}{2} I_{2-2} \dot{\theta}^2 + \frac{1}{2} I_{1-1} \dot{\phi}^2$$

substituting for  $\dot{\theta}$  and  $\dot{\phi}$  their values,  $0.11124 \times 10^{-2}$  and  $0.151 \times 10^{-2} \text{ sec}^{-1}$  respectively, we obtain;

$E_{sh} = 29.96 + 6.69 + 0.616 = 37.26 \text{ (ton} \cdot \text{m)}$

Structure

$$E_s = \frac{1}{2} M_1 \cdot \dot{S}^2 = \frac{1}{2} \times 0.7 \times (-4.659)^2 / 100 = 0.077 \text{ (ton} \cdot \text{m)}$$

$E_{sh} + E_s = 37.26 + 0.077 = 37.3 \text{ (ton} \cdot \text{m)}$

Total energy at  $V_c = 0.0$  will be;

$E_e + E_{sh} + E_s = 79.09 \text{ (ton} \cdot \text{m)} \dots\dots(39)$

But the ship's approaching energy is;

$$E_0 = \frac{1}{2} \times 70.69 \times 15^2 / 100 = 79.520 \text{ (ton} \cdot \text{m)} \dots\dots(40)$$

Eq. (39)  $\div$  Eq. (40) which satisfied the conservation of kinetic energy before and collision.

2) Conservation of the moment of momentum

i) At time when the ship made the first contact, the moment of momentum is given by;

$$MM_1 = M_2 \cdot V_0 \cdot r \sin \gamma = 70.69 \times 15 \times 8000 \times 0.766 / 100 = 649.8 \times 10^3 \text{ (ton} \cdot \text{sec} \cdot \text{m)} \dots\dots(41)$$

ii) At time when the ship started to rebound, the moment of momentum is equal to;

$$MM_2 = I_{2-2} \dot{\theta} + I_{1-1} \dot{\phi} + M_2 \sqrt{\dot{X}_G^2 + \dot{Y}_G^2} \cdot r = 126.10 \times 10^3 + 8.15 \times 10^2$$

$$\begin{aligned}
 &+527.80 \times 10^2 \\
 &=662.05 \times 10^2 \text{ (ton}\cdot\text{sec}\cdot\text{m)} \\
 &\dots\dots(42)
 \end{aligned}$$

Eq. (41)=Eq. (42) which satisfied the moment of momentum principles.

(2) Checking of Time Interval Selection Procedure

The accuracy of the deduced results, as seen in the previous paragraph, verified, on one hand, the right procedure of developing the equations of motion, and on the other hand, it supported the author's recommendations for the evaluation of the time interval  $\Delta T$  presented in section 4. Fig. 18 shows the variation of  $\Delta T$  through the numerical integration process according to the variation of the fender's stiffness shown by Fig. 17. Any mis-choice of the time interval will lead to large errors, and sometime, leads to unreasonable results as included in Table 4.

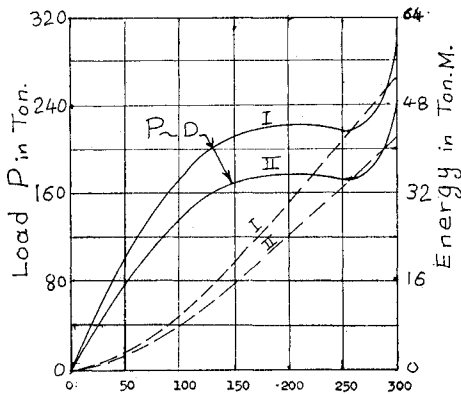


Fig. 17 The load and energy vs. deflection for V600H rubber fender (Tokyo Rubber Dock Fenders).

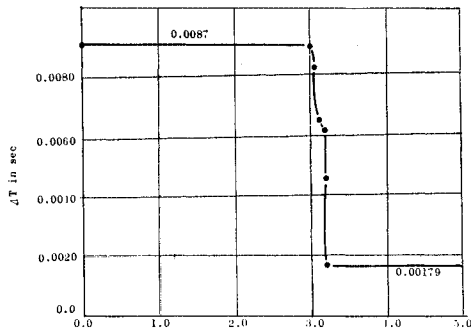


Fig. 18 Variation of time interval  $\Delta T$  vs. time of berthing.

7. COMPARING THE METHOD WITH OTHER INVESTIGATORS METHOD

i) Case 2, Table 5, in which  $H=0.0$ , is similar to the case treated by Vasco Costa, *i.e.* swaying and yawing motions are only considered. From the table we have; at  $V_C=0.69 \div 0.0$  cm/sec.

$$\begin{aligned}
 E_e &= (V_{sz} + V_{sy} + V_f) = (18.40 + 3.42 + 20.27) \\
 &= 42.09 \text{ (ton/m)} \dots\dots(43)
 \end{aligned}$$

Substituting with the given data in the equation given by Vasco Costa, we obtain;

$$\begin{aligned}
 E_e &= (W) = \frac{1}{2} M_2 V_0 \frac{k_0^2 + r^2 \cos^2 \gamma^2}{k^2 + r^2} \\
 &= 42.15 \text{ (ton/m)} \dots\dots(44)
 \end{aligned}$$

ii) Case 3 is similar to the case treated by Hayashi & Shirai, *i.e.* fender of linear spring constant and  $\gamma$ , Fig. 1, equals to  $90^\circ$ .

From i) and ii), if we considered some error due to numerical integration, the author's method will be in agreement with the two special cases treated in references 4) and 5).

8. SUMMARY AND CONCLUSIONS

The foregoing study describes an analytical treatment of the ship berthing problem, based on the dynamic response of the ship and the fender system during berthing.

The presented analysis covers almost the main factors involving in berthing operations. These are comprised of;

- i) The approaching mode of the ship with reference to the face of the berth, designed by  $\alpha$  and  $\gamma$ .
- ii) The location of the point of contact on the ship's hull, denoted by  $r$  and  $H$ .
- iii) The structure stiffness and the fender stiffness, whether the latter of a linear or non-linear spring constant, beside to the hull stiffness at the point of contact, if available.
- iv) The mechanical behaviour of the fender system with respect to the variation of the acting load direction. This is very important in case of rubber-like fenders, as their energy absorbing capacity is a function of the load direction.
- v) Consideration of shallow water effect in swaying, yawing and rolling.

For solving the developed equations of motions, recommendations and formulas for estimation and selection of the different parameters, particularly the time interval, are presented.

The solution of these equations will lead to the evaluation of the data required for designing the fender system;

- i) Evaluation of the energy absorbed by the fender.
- ii) Evaluation of the energy absorbed by the fender structure and its dynamic reaction, magnitude and direction.

#### REFERENCES

- 1) James Michalos: "Dynamic Response and Stability of Piers on Piles", ASCE Proc. Paper 3221, August 1962, Vol. 87, WW2.
- 2) James Michalos and David P. Billington: "Design and Stability Consideration for Unique Pier", ASCE Proc. Paper 2807, May 1961, Vol. 87, WW2.
- 3) Lymon C. Reese: Discussion on Paper 3221, Reference 1) ASCE Proc. Discussion, May 1963, WW2.
- 4) T. Hayashi and M. Shirai: Force of Impact at the Moving Collision of a Ship with the Mooring Construction, Coastal Eng. in Japan, Vol. 6, 1963.
- 5) F. Vasco Costa: "The Berthing Ship", Dock and Harbour Authority, Vol. 45, No. 523, May 1964, No. 524, June 1964 and No. 525, July 1964.
- 6) Theodore T. Lee: "Design Criteria Recommended for Marine Fender Systems", Proceeding of Eleventh Conf. on Coastal Eng., Vol. 1, Part 2, 1968.
- 7) Lymon Reese and Michael W.: "Rational Design Concept for Berthing Dolphins", ASCE Proc. Paper 7291, May 1970, WW2.
- 8) B. G. Tyrrell: "Mooring Dolphins", Dock and Harbour Authority, Part 1, August 1966, pp. 115-120, Part 2, September 1966, pp. 161-166.
- 9) Vasco Costa: "Berthing Manoeuvres of Large Ships", Dock and Harbour Authority, March 1968, pp. 351-358.
- 10) "The Construction of Quays and Jetties," Dock and Harbour Authority, Vol. 42, April 1962.
- 11) Shu-t'ien Li: "Operative Energy Concept in Marine Fendering", ASCE Proc. Paper 2875, August 1961, Vol. 87, No. WW3.
- 12) F. H. Todd: Ship Hull Vibration, Edward Arnold L. T. London, 1961, pp. 65-104.
- 13) Y. Matsuura and H. Kawakami: "Calculation of Added Virtual mass of inertia of ship", Journal of Zosen Kiokai, J.S.N.A., November 1968. (In Japanese)
- 14) Y. Matsuura, H. Kawakami and H. Onogi: "Study on the Coupled Torsional and Flex-tual Vibrations of Ships," Journal of Kansai Zosen Kiokai, September 1969. (In Japanese)
- 15) T. Sawamura: "The Determination of the Breadth of Ship Coupling GM and  $D/d$  ratio," Journal of Zosen Kiokai, J.S.N.A., December 1965. (In Japanese)
- 16) Nathan M. Newmark: A Method of Computation for Structural Dynamics", ASCE Proc. Struct. Div. Paper 2094, July 1959.
- 17) Norris and Others: "Structural Design for Dynamic Loads", McGraw-Hill Book Co., 1959, pp. 183-212.
- 18) H. W. Reeves: "Marine Oil Terminal for Rio de Janeiro, Brazil", ASCE, Proc., Vol. 87, February 1961, WW1.
- 19) T. Kumai: "Some Correction Factors for Virtual Inertia Coefficient on the Horizontal Vibration of a Ship", Journal of Zosen Kiokai, J.S.N.A., Vol. 108, 1960.

(Received Sept. 2, 1971)